

Molecular Generation with Recurrent Neural Networks

Esben Jannik Bjerrum*

June 8, 2022

Wildcard Pharmaceutical Consulting, Frødings Allé 41, 2860 Søborg, Denmark
*) esben@wildcardconsulting.dk

Abstract

The potential number of drug like small molecules is estimated to be between 10^{23} and 10^{60} while current databases of known compounds are orders of magnitude smaller with approximately 10^8 compounds. This discrepancy has led to an interest in generating virtual libraries using hand crafted chemical rules and fragment based methods to cover a larger area of chemical space and generate chemical libraries for use in *in silico* drug discovery endeavors. Here it is explored to what extent a recurrent neural network with long short term memory cells can figure out sensible chemical rules and generate synthesizable molecules by being trained on existing compounds encoded as SMILES. The networks can to a high extent generate novel, but chemically sensible molecules. The properties of the molecules are tuned by training on two different datasets consisting of fragment like molecules and drug like molecules. The produced molecules and the training databases have very similar distributions of molar weight, predicted logP, number of hydrogen bond acceptors and donors, number of rotatable bonds and topological polar surface area when compared to their respective training sets. The compounds are for the most cases synthesizable as assessed with SA score and Wiley ChemPlanner.

Introduction

The number of potential drug like molecules is huge due to the large flexibility and combinatorial potential of organic carbon, nitrogen and oxygen chemistry. The number has been estimated to be between 10^{23} and 10^{60} [1, 2, 3] and dwarfs the current largest databases of chemical compounds, such as ChemBL[4]: $\sim 2 \times 10^6$, PubChem[5] $\sim 90 \times 10^6$ and ChemSpider[6] $\sim 60 \times 10^6$. It has therefore long been of interest to generate virtual chemical libraries for *in silico* drug discovery purposes[7]. A strategy for generation of a virtual library can be enumeration of products from reaction of libraries of fragments, which ensures the synthetic feasibility of the product and the availability of the reaction fragments can be taken into account[8]. Examples of software solutions to enumerate such collections are eSynth[9] and iLibDiverse built upon CombiGen[10], and there are also already

developed databases available such as the GDB sets[11, 12, 13]. Many pharmaceutical companies have also developed solutions to enumerate compounds that are within their synthetic reach and/or covered by their current patents, thus defining a chemical space of compounds which known synthetic routes and intellectual property coverage[14, 15].

Deep Neural Networks has gained a lot of interest for their ability to do feature extraction and learn rules from presented training data. The availability of GPU's and CUDA enabled back-ends makes prolonged training available at a modest cost. New regularization schemes such as dropout[16] and noise layers[17] has enables larger and deeper network architectures without extensive over fitting. Task oriented architectures such as convolutional neural networks[18] (CNN) for spatial related data such as images, has led to improvements in image analysis whereas recurrent neural networks[19] (RNNs) have shown

success for sequence based input. In RNNs, the state of the network is propagated forward for each step of the input sequence, enabling the network to alter its internal state for each input step and thus alter the output even though the weights are the same in the network. The performance of RNNs has seen huge improvements with use of micro architectures such as long short term memory (LSTM)[20] cells and gated recurrent units (GRU)[19]. LSTM cells are a pre configured micro architecture of a neural network, which has controlled gates for input, forget and output. This enables the unit to keep its internal state for longer stretches of sequential input in the recurrent neural network, leading to an improvement of the recurrent neural network performance. The cells can be combined and stacked into architectures that have interesting properties with regard to analysis of textual or sequence based inputs.

An interesting property of RNN's is their ability to be played forward and generating new sequences[21]. This is done in an iterative manner where the predicted character or next step in the sequence are fed back into the recurrent neural network, altering its state and leading to a new prediction for the next step in the sequence. For molecules it is possible to describe the full configuration of atoms and connection using the condensed SMILES notation[22]. Letters and special characters are used to describe the topology of the molecules. Here an RNN is applied to datasets of SMILES strings, enabling the generation of virtual compound libraries. The molecular properties of the novel virtual molecules are investigated and compared with the training datasets and the synthetic feasibility evaluated by scoring and retrosynthetic analysis.

Methods

Datasets

The clean drug like (p13) and the clean fragments subset (p12) was downloaded in SMILES[22] format from the Zinc12[23, 24] website and unzipped. The order of the lines was shuffled with the GNU core utilities[25] shuf command line tool. A custom Python[26] script was used to prefix the SMILES with a start character “!” and padded with an end character “E” to a fi-

nal length two characters longer than the longest SMILES string in the set. The SMILES sets were subsequently vectorized by one hot encoding into HDF5[27] data files. The character to index translation information were saved for each dataset.

Neural Network

A recurrent neural network was built using Keras[28] with Theano[29] as computation back end. First two layers were constructed of 256 LSTM[20] units run in batch mode with an input layer matching the number of vectorized characters and the length of the padded SMILES. This was followed by a time distributed feed forward network consisting of two hidden layers with 128 neurons with rectified linear activation. The final output layer matched the number of characters in the dataset index with a soft-max activation. The LSTM units were regularized with an input dropout[16] of 0.1 (dropout_W).

The neural network were trained by reading chunks of 100.000 vectorized SMILES into memory which were used in mini-batches of 512 for one epoch of training for each chunk. The first chunk was reserved for use as validation set during training. Learning rate was initially set to 0.007 but gradually lowered if the validation loss did not improved within the last 5 chunks of training.

Sampling

A sampling model was built with the exact same architecture as the training model, except the LSTM layers were run in stateful mode instead of batch mode and the input dimension set to a vector size of the number of characters in the dataset vectorization dictionary. The output probabilities was adjusted with a sampling temperature, that rescales the probabilities in the output vector with the following formula:

$$p_{new} = e^{\ln(\frac{p_{ori}}{temp})}$$

Final selection of the next character was then done with numerical Pythons multinomial sampler. The networks state was reset before SMILES generation and the initial character fed to the network was the start character “!”. Sampling was terminated when the end character “E”

was predicted. The start and end characters were stripped and the SMILES molecular validity checked by conversion to a sanitized molecule with RDKit[30].

Two datasets of 50.000 molecules were generated with both trained models using a sampling temperature of 1.0. Using RDKit, they were converted to canonical SMILES, as was the training sets. The number of similar molecules was found by intersecting the generated set with the corresponding full training set.

Calculation of Molecular Properties

The two generated datasets were compared with random samples of 50.000 molecules of both training sets. RDKit was used to calculate a range of molecular properties: the number of hydrogen bond acceptors, number of hydrogen bond donors, total polar surface area, number of rotatable bonds and the molecular weight as well as the predicted LogP[31]. In addition, the SA-score[32] was calculated on compounds with the sascorer module from the RDKit SA_score contribution package. The compounds were converted to neutral form with the MolVS package[33] before the SA score was computed. Comparison plots were made with Matplotlib[34].

All computations and training were done on a Linux workstation (Ubuntu Mate 16.04) with 4 GB of ram, i5-2405S CPU @ 2.50GHz and an Nvidia Geforce GTX1060 graphics card with 6 GB of ram.

Retrosynthetic analysis

Compounds were selected for retro-synthetic analysis by sampling the 10 compounds nearest the 5, 50 and 95% percentile of the SA score distribution as well as the compound with the highest SA score. Compounds already found in the training sets were discarded. Each compound were subjected to retro-synthetic analysis with the Wiley ChemPlanner software[35] at default settings. Longest linear route to intermediates were 3 steps and common reaction rules were employed. Routes were completed until commercially available starting materials with a cost less than 1000\$/mol were found. If no commercially available starting materials were found with the default settings, the max number of linear steps

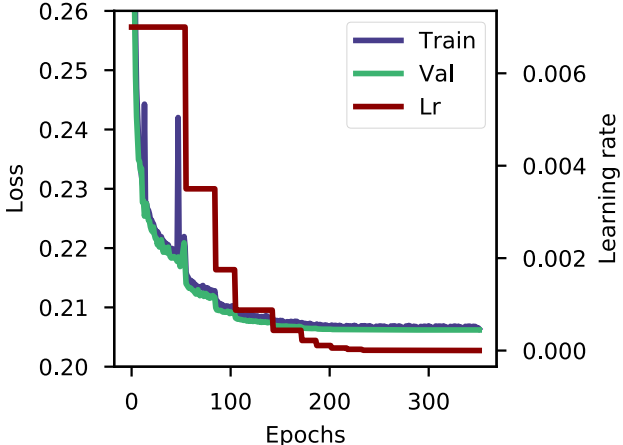


Figure 1: Training History for the p12 dataset (fragment like).

was increased to 4. If no feasible routes could be found, the starting materials found in the first round of retro-synthetic planning were submitted to up to two more retrosynthetic planning sessions using rare chemical synthetic rules.

Results

Training was done for 352 chunks for p12 (fragment like) and 449 chunks for p13 (drug like). The training history for p12 are shown in Figure 1. The training history for p13 looks essentially similar (not shown), although a slightly lower final validation loss of 0.167 was obtained. As p12 contains 1.611.889 SMILES and p13 was 13.195.609, this corresponds to approximately 22 and 3.5 passes over the entire datasets, respectively. The difference between the validation loss and training loss were negligible for both datasets.

Examples of the molecules generated with the model trained on drug like molecules are shown in Figure 2. At a glance there seem to be correctly made 6 membered benzene rings and some 5 membered heterocyclic rings which makes electronic sense according to RDKit. Fused ring systems are also present. Nitrogens in amides and near aromatic rings appear uncharged, whereas primary and secondary aliphatic amines are charged, reflecting the charge normalization of the training set done by the Zinc database. The molecules generated from the model trained on fragments on average appear to be smaller and more simple (Figure 3).

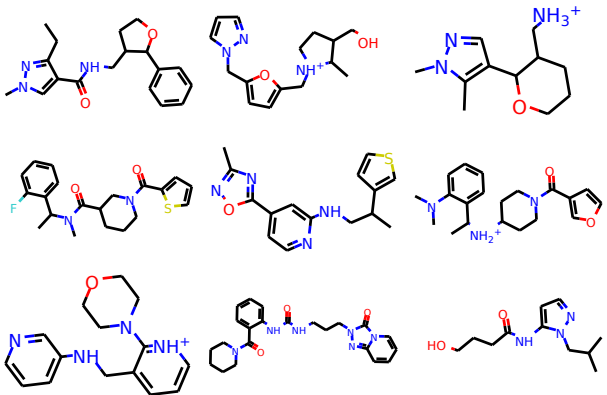


Figure 2: Examples of generated molecules from the model trained on drug like molecules (p13).

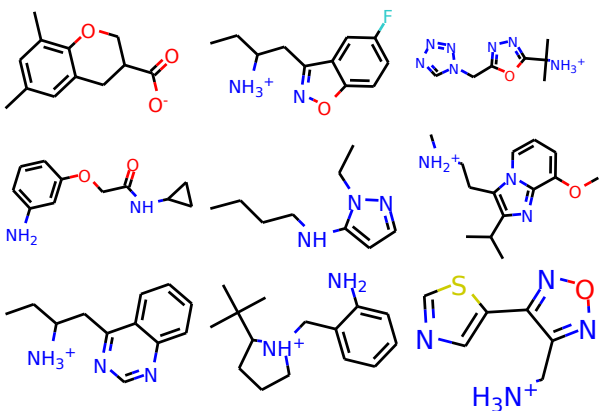


Figure 3: Examples of molecules generated from the model trained on the dataset with molecular fragments (p12).

Some of the generated SMILES strings were malformed during sampling and could not be parsed with RDKit. The fraction of the molecules which contains errors was dependent on the sampling temperature with approximately 2% being malformed at a temperature of 1.0 (Figure 4). At temperatures over 1.2 the error rate rises significantly. Typical errors preventing SMILES parsing was missing closure of parentheses or unmatched ring closures. Occasionally the valence of atoms were wrong.

37% of the generated fragments was found in the training set, whereas only 17% of the generated drug-like molecules were found in the training set.

Comparison of molecular features

The properties of the molecules generated matches the properties of the molecules used for

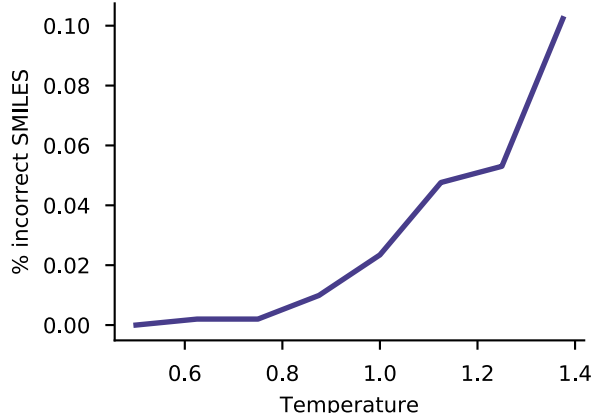


Figure 4: Molecular sampling error at different sampling temperature. High sampling temperatures leads to malformed SMILES strings.

training of the neural networks. Figure 5 show the histograms of the properties for both samples of the training sets and generated sets. The distribution of the properties of the generated molecules to a large extent overlaps with the distribution found in the two training sets. The differences between the two training sets reflects the filtering done by the Zinc database to define the dataset. The fragments are defined as molecules with $xlogp \leq 3.5$ and $mwt \leq 250$ and rotatable bonds ≤ 5 , whereas the drug like molecules have a molar weight between 150 and 500, $xlogp \leq 5$ and the number of rotatable bonds ≤ 7 . Additionally the drug like molecules must have a polar surface area below 150, number of hydrogen bond donors ≤ 5 and number of hydrogen bond acceptors ≤ 10 . The difference between the two datasets are most pronounced for the molecular weight histograms, where the filtering of the training sets are evident as sharp cutoffs in the histograms. The generated training sets follow this sharp edge only partially, but also generates a few molecules with a larger molecular weight than found in the training sets as evident from the thin tails.

The synthetic feasibility of the generated molecules seem to very closely follow the training sets as assessed by the synthetic accessibility score[32] (SA-score Figure 6) This score uses a combination of fragment contributions and assessed topological complexity of the molecule, such as presence of unusual ring systems, stereo complexity and molecular size[32]. The distributions of the generated and training sets are essen-

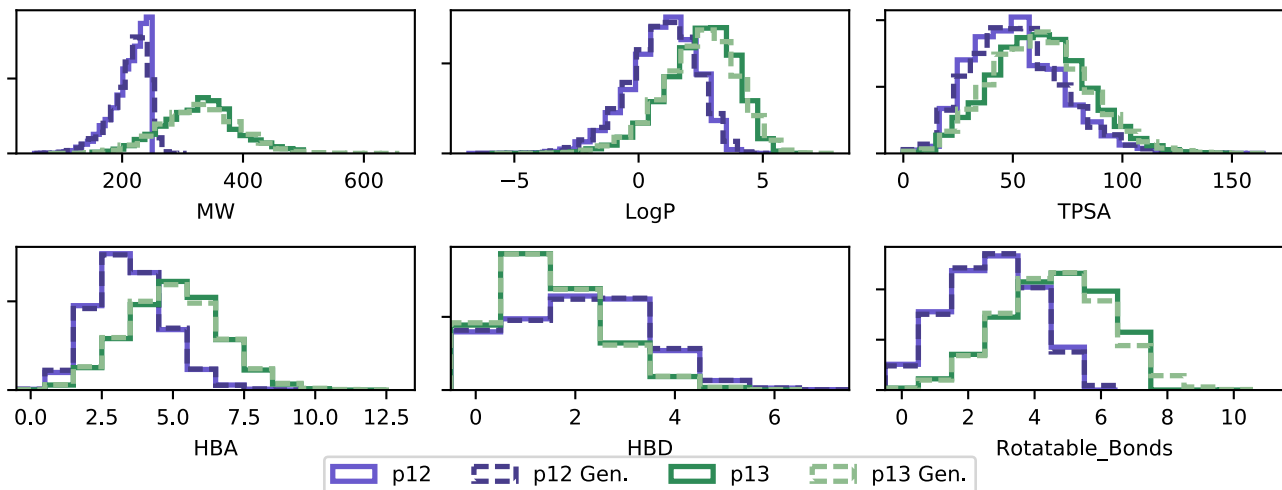


Figure 5: Calculated property distributions of the generated molecules. The generated molecules distribution of properties (dashed lines) matches the training sets (solid lines) used for all calculated properties: Molecular weight (MW), calculated LogP (LogP), total polar surface area (TPSA), number of hydrogen bond acceptors (HBA), number of hydrogen bond donors (HBD) and number of rotatable bonds. p12 and p13 are the Zinc sets for clean fragments and clean drug like molecules, respectively.

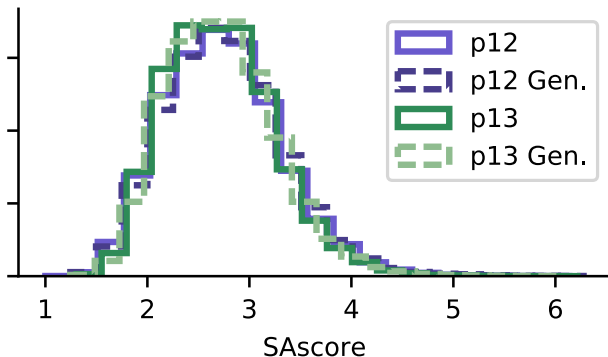


Figure 6: SA-score distribution for 50.000 compound samples of generated molecules and training sets. The generated molecules SA-scores closely follows the SA-score of their respective training sets. p12 and p13 are clean fragments and clean drug-like molecules respectively.

tially similar.

To further investigate the synthesizability of the generated molecules, three groups of compounds were selected from the drug-like molecules based on their SA score. A summary of the properties of the identified synthetic rules for each group are shown in Table 1. ChemPlanner found retro-synthetic routes for all compounds in the easy group with the default settings. For the medium group, possible problems were noted for two out of 6 selected compounds, and the second highest ranked route was chosen for one of

them. A route to one of the compounds in the hard group could not be established, even though the number of steps was increased as well as using more rare reactions. Moreover, for the compound with the highest SA score, no route was identified from commercially available starting materials. The summary in Table 1 illustrates the expected differences between the groups. The highest proportion of possible selectivity issues were found in the group with the highest SA score, as well as this group required the most steps, gave the lowest yield and had the highest average cost of the starting material. The number of synthetic routes were larger for the hard group possibly reflecting the larger amount of combinations for longer synthetic routes with more intermediates. The full table with details on each sampled compound can be found in the Supplementary Information.

Discussion

The most obvious question to ask of the automatically created novel molecules are regarding their practical synthesizability. The created compounds complexity, topology and created fragments closely matches the ones found in the training set, which are already synthesized compounds. The calculated SA score thus seem to match very closely and is in the easy to medium

Table 1: Average properties of the retro-synthetic routes found by ChemPlanner for three groups sampled near the 5, 50 and 95% percentiles of the SA score distribution

Group	Possible Selectivity Issues	SA Score	No. of synthesis routes	Max steps	Yield / %	Cost of SMs US\$/100g
Easy	0/6	1.9	26.0	2.2	55.7	1043.8
Medium	1/6	2.7	40.0	3.7	35.2	1690.8
Hard	4/9	3.7	42.1	4.4	26.1	1717.3

end of the range observed for molecules, and matches the SA scores observed for catalog compounds in the original study[32]. Using Wiley ChemPlanner[35], three groups of molecules were subjected to retro-synthetic planning, were for the majority of compound retro-synthetic routes could be identified (c.f. Table 1). There seemed to be a larger proportion of possible problems with compounds from the group with the highest SA scores, indicating that the SA score could be used as a first screen of the generated compound before further detailed evaluation if synthesizability feasibility and cost is an issue. The SA scores is however in the medium to low range when compared to the scores reported[32], illustrating that for all except the easiest cases, the compounds should be more detailed evaluated by retro-synthetic software[35] or trained medicinal chemists.

The sampling provided novel molecules not found in the training set, 63% and 83% for the fragment like and drug like sets respectively. The larger drug like molecules were more novel, even if the training set was almost an order of magnitude larger and thus representing a larger sampling set in which to re find a given molecule. This is possibly due to a larger possible combinatorial space for the atomic connections of the molecules. Considering the large estimated numbers of drug like molecules (vide supra), it is surprising that the recurrent network generates such a large proportion of molecules already found in the training sets. This indicates over fitting of the networks, which is not apparent from the training graphs, Figure 1, and the similarity of the final loss function from the training and test set. This could reflect that the training and test sets are too similar in properties: The original database could contain a high proportion of compound series that have been split into both the training

and test sets. This effect could possible be mitigated by performing a clustering based on scaffolds as encoded by circular fingerprints followed by a division into training and test set based on clusters. This could ensure a setting of hyper parameters that makes the networks cover more diverse areas of chemical space. As it is now, the networks seem to only generates molecules in the vicinity of the training molecules, leading only to a small expansion of the chemical space covered.

On the other hand, this propensity to generate molecules in the vicinity of the training sets, could be used to generate molecules similar to known actives. However, the small size of the datasets with known actives easily leads to extensive over fitting, although limited re-training of previously trained networks seems promising[36]. Techniques such as data augmentation with SMILES enumeration could also be of potential use[37]. A recent publication used a similar approach with reinforcement learning to tune a generative recurrent neural network for producing molecules and additionally demonstrated how the network could be tuned towards generating molecules of potential bio activity[38].

The close link between the training set and the generated molecules could potentially lead to interesting iterative approaches in *in silico* drug discovery resembling genetic algorithms. The network could be used to generate a set of molecules which are subsequently evaluated with QSAR models or molecular docking. The best half is then used to retrain the network. After a couple of cycles the produced molecules would likely have better properties in the *in silico* models.

Conclusion

Recurrent neural networks with LSTM cells can be trained to generate novel and chemically plausible molecules as assessed by SA score and retrosynthetic analysis with Wiley ChemPlanner. The distribution of the molecular properties of the generated molecules closely resembles the property distributions in the used training sets, making it possible to tune the networks by filtering the datasets. This possibility leads to novel possibilities for expanding known compound series with similar compounds of matched properties for generation of larger in silico compound libraries. There was a correspondence between the SA score and the properties of the retro-synthetic routes, although no routes could be found for two of the compounds selected for detailed analysis.

Acknowledgements

Wiley ChemPlanner is thanked for providing free testing of their retro-synthetic algorithms and Dr. Richard Threlfall for help with the software <http://www.chemplanner.com>

Conflict of interests

E. J. Bjerrum is the owner of Wildcard Pharmaceutical Consulting. The company is usually contracted by biotechnology/pharmaceutical companies to provide third party services

References

- [1] P. G. Polishchuk, T. I. Madzhidov, A. Varnek, Estimation of the size of drug-like chemical space based on gdb-17 data., *Journal of computer-aided molecular design* 27 (2013) 675–679. doi:10.1007/s10822-013-9672-4.
- [2] P. Ertl, Cheminformatics analysis of organic substituents: identification of the most common substituents, calculation of substituent properties, and automatic identification of drug-like bioisosteric groups., *Journal of chemical information and computer sciences* 43 (2003) 374–380. doi:10.1021/ci0255782.
- [3] R. S. Bohacek, C. McMartin, W. C. Guida, The art and practice of structure-based drug design: a molecular modeling perspective., *Medicinal research reviews* 16 (1996) 3–50. doi:10.1002/(SICI)1098-1128(199601)16:1<3::AID-MED1>3.0.CO;2-6.
- [4] A. P. Bento, A. Gaulton, A. Hersey, L. J. Bellis, J. Chambers, M. Davies, F. A. KrÃŒger, Y. Light, L. Mak, S. McGlinchey, M. Nowotka, G. Papadatos, R. Santos, J. P. Overington, The chembl bioactivity database: an update., *Nucleic acids research* 42 (2014) D1083–D1090. doi:10.1093/nar/gkt1031.
- [5] S. Kim, P. A. Thiessen, E. E. Bolton, J. Chen, G. Fu, A. Gindulyte, L. Han, J. He, S. He, B. A. Shoemaker, J. Wang, B. Yu, J. Zhang, S. H. Bryant, Pubchem substance and compound databases., *Nucleic acids research* 44 (2016) D1202–D1213. doi:10.1093/nar/gkv951.
- [6] H. E. Pence, A. Williams, Chemspider: an online chemical information resource (2010).
- [7] Leach, Hann, The in silico world of virtual libraries., *Drug discovery today* 5 (2000) 326–336.
- [8] M. Hartenfeller, G. Schneider, De novo drug design., *Methods in molecular biology* (Clifton, N.J.) 672 (2011) 299–323. doi:10.1007/978-1-60761-839-3_12.
- [9] M. Naderi, C. Alvin, Y. Ding, S. Mukhopadhyay, M. Brylinski, A graph-based approach to construct target-focused libraries for virtual screening., *Journal of cheminformatics* 8 (2016) 14. doi:10.1186/s13321-016-0126-6.
- [10] G. Wolber, T. Langer, Combigen: A novel software package for the rapid generation of virtual combinatorial libraries, *Rational Approaches to drug design* (2001) 390–399.
- [11] T. Fink, J.-L. Reymond, Virtual exploration of the chemical universe up to 11 atoms of c, n, o, f: assembly of 26.4 million structures (110.9 million stereoisomers) and analysis for new ring systems, stereochemistry, physicochemical properties, compound

classes, and drug discovery, *Journal of chemical information and modeling* 47 (2) (2007) 342–353.

[12] L. Ruddigkeit, R. Van Deursen, L. C. Blum, J.-L. Reymond, Enumeration of 166 billion organic small molecules in the chemical universe database gdb-17, *Journal of chemical information and modeling* 52 (11) (2012) 2864–2875.

[13] L. C. Blum, J.-L. Reymond, 970 million druglike small molecules for virtual screening in the chemical universe database gdb-13, *Journal of the American Chemical Society* 131 (25) (2009) 8732–8733.

[14] C. A. Nicolaou, I. A. Watson, H. Hu, J. Wang, The proximal lilly collection: Mapping, exploring and exploiting feasible chemical space., *Journal of chemical information and modeling* 56 (2016) 1253–1266. doi: 10.1021/acs.jcim.6b00173.

[15] Q. Hu, Z. Peng, S. C. Sutton, J. Na, J. Kostrowicki, B. Yang, T. Thacher, X. Kong, S. Mattaparti, J. Z. Zhou, J. Gonzalez, M. Ramirez-Weinhouse, A. Kuki, Pfizer global virtual library (pgvl): a chemistry design tool powered by experimentally validated parallel synthesis information., *ACS combinatorial science* 14 (2012) 579–589. doi:10.1021/co300096q.

[16] N. Srivastava, G. E. Hinton, A. Krizhevsky, I. Sutskever, R. Salakhutdinov, Dropout: a simple way to prevent neural networks from overfitting., *Journal of Machine Learning Research* 15 (1) (2014) 1929–1958.

[17] Y. Luo, F. Yang, Deep learning with noise (2014).
URL <http://www.cs.cmu.edu/~fanyang1/dl-noise.pdf>

[18] P. Y. Simard, D. Steinkraus, J. C. Platt, et al., Best practices for convolutional neural networks applied to visual document analysis., in: ICDAR, Vol. 3, Citeseer, 2003, pp. 958–962.

[19] J. Chung, C. Gulcehre, K. Cho, Y. Bengio, Empirical evaluation of gated recurrent neu-

ral networks on sequence modeling, *arXiv preprint arXiv:1412.3555*.

[20] S. Hochreiter, J. Schmidhuber, Long short-term memory, *Neural computation* 9 (8) (1997) 1735–1780.

[21] I. Sutskever, J. Martens, G. E. Hinton, Generating text with recurrent neural networks, in: *Proceedings of the 28th International Conference on Machine Learning (ICML-11)*, 2011, pp. 1017–1024.

[22] D. Weininger, Smiles, a chemical language and information system. 1. introduction to methodology and encoding rules, in: *Proc. Edinburgh Math. SOC*, Vol. 17, 1970, pp. 1–14.

[23] J. J. Irwin, B. K. Shoichet, Zinc—a free database of commercially available compounds for virtual screening., *Journal of chemical information and modeling* 45 (2005) 177–182. doi:10.1021/ci049714+.

[24] J. J. Irwin, T. Sterling, M. M. Mysinger, E. S. Bolstad, R. G. Coleman, Zinc: a free tool to discover chemistry for biology, *Journal of chemical information and modeling* 52 (7) (2012) 1757.

[25] Gnu, <https://www.gnu.org> (2017).

[26] G. Van Rossum, F. L. Drake Jr, *Python reference manual*, Centrum voor Wiskunde en Informatica Amsterdam, 1995.

[27] The HDF Group, Hierarchical data format version 5 (2000-2010).
URL <http://www.hdfgroup.org/HDF5>

[28] F. Chollet, keras, <https://github.com/fchollet/keras> (2015).

[29] R. Al-Rfou, G. Alain, A. Almahairi, C. Angermueller, D. Bahdanau, N. Ballas, F. Bastien, J. Bayer, A. Belikov, A. Belopolsky, Y. Bengio, A. Bergeron, J. Bergstra, V. Bisson, J. Bleecher Snyder, N. Bouchard, N. Boulanger-Lewandowski, X. Bouthillier, A. de Brébisson, O. Breuleux, P.-L. Carrier, K. Cho, J. Chorowski, P. Christiano, T. Cooijmans, M.-A. Côté, M. Côté,

A. Courville, Y. N. Dauphin, O. Delalleau, J. Demouth, G. Desjardins, S. Dieleman, L. Dinh, M. Ducoffe, V. Dumoulin, S. Ebrahimi Kahou, D. Erhan, Z. Fan, O. Firat, M. Germain, X. Glorot, I. Goodfellow, M. Graham, C. Gulcehre, P. Hamel, I. Harlouchet, J.-P. Heng, B. Hidasi, S. Honari, A. Jain, S. Jean, K. Jia, M. Korobov, V. Kulkarni, A. Lamb, P. Lamblin, E. Larsen, C. Laurent, S. Lee, S. Lefrancois, S. Lemieux, N. Léonard, Z. Lin, J. A. Livezey, C. Lorenz, J. Lowin, Q. Ma, P.-A. Manzagol, O. Mastropietro, R. T. McGibbon, R. Memisevic, B. van Merriënboer, V. Michalski, M. Mirza, A. Orlandi, C. Pal, R. Pascanu, M. Pezeshki, C. Raffel, D. Renshaw, M. Rocklin, A. Romero, M. Roth, P. Sadowski, J. Salvatier, F. Savard, J. Schlüter, J. Schulman, G. Schwartz, I. V. Serban, D. Serdyuk, S. Shabanian, E. Simon, S. Spieckermann, S. R. Subramanyam, J. Sygnowski, J. Tanguay, G. van Tulder, J. Turian, S. Urban, P. Vincent, F. Visin, H. de Vries, D. Warde-Farley, D. J. Webb, M. Willson, K. Xu, L. Xue, L. Yao, S. Zhang, Y. Zhang, Theano: A Python framework for fast computation of mathematical expressions, arXiv e-prints abs/1605.02688.
URL <http://arxiv.org/abs/1605.02688>

[30] G. A. Landrum, Rdkit: Open-source cheminformatics software (2016).
URL <http://www.rdkit.org/>, <https://github.com/rdkit/rdkit>

[31] S. A. Wildman, G. M. Crippen, Prediction of physicochemical parameters by atomic contributions, Journal of chemical information and computer sciences 39 (5) (1999) 868–873.

[32] P. Ertl, A. Schuffenhauer, Estimation of synthetic accessibility score of drug-like molecules based on molecular complexity and fragment contributions., Journal of cheminformatics 1 (2009) 8. doi:10.1186/1758-2946-1-8.

[33] M. Swain, Molvs, GitHub (May 2017).
URL <https://github.com/mcs07/MolVS>

[34] J. D. Hunter, Matplotlib: A 2d graphics environment, Computing In Science & Engineering 9 (3) (2007) 90–95. doi:10.1109/MCSE.2007.55.

[35] Wiley chemplanner, <http://www.chemplanner.com/> (2017). URL <http://www.chemplanner.com/>

[36] Teaching computers molecular creativity, <http://www.wildcardconsulting.dk/useful-information/teaching-computers-molecular-creativity/> Accessed November 2016 (Nov 2016). URL <http://www.wildcardconsulting.dk/useful-information/teaching-computers-molecular-creativity/>

[37] E. J. Bjerrum, Smiles enumeration as data augmentation for neural network modeling of molecules, arXiv preprint arXiv:1703.07076.

[38] M. Olivecrona, T. Blaschke, O. Engkvist, H. Chen, Molecular de novo design through deep reinforcement learning, arXiv preprint arXiv:1704.07555.